Olson ENGINEERING
Corporate Office:
12401 W. 49th Avenue
Wheat Ridge, CO 80033 USA
phone: 303.423.1212
fax: 303.423.6071

Non-Destructive Evaluation (NDE) for Condition Assessment of Concrete Dams

Larry D. Olson, PE[1]
Lyndsay A. Hazelwood[2]

Presented: May 18, 2021 at the 2021 USSD Annual Conference
Published: May 18, 2021

ABSTRACT

There are a number of nondestructive evaluation (NDE) methods applicable to investigations into the condition of concrete dam structures. Included in this paper is a discussion of the methods themselves and the applicability of the methods to different types of dams and structures related to dams, as well as several case histories of the methods in application. The NDE methods to be discussed include Spectral Analysis of Surface Waves, Impact Echo, Ground Penetrating Radar, Slab Impulse Response, and Sonic Velocity Cross-Dam Tomography for imaging conditions inside concrete dams. The methods are applicable to a variety of concrete elements found on many types of dams. These elements include spillway concrete evaluation, spillway subgrade evaluation, dam wall concrete evaluation, and thin-arch dam interior evaluation. Several of the techniques discussed can be applied from the downstream face of a thin-arch concrete dam to evaluate the condition of the concrete through the entire cross-section with no dewatering required. In fact, the Cross Dam Tomography method works best when the dam is as full as possible. Conditions evaluated include freeze-thaw damage, cracking, general concrete quality, and void. The results of the nondestructive evaluation investigation aid in planning repairs and evaluating dam safety. The applications of the NDE methods are illustrated in case histories from several concrete dams.

INTRODUCTION

As the world's dam infrastructure ages, it becomes increasingly important to be able to determine the condition of existing dam facilities and track changes in condition over time. This is especially true for critical dam infrastructure elements such as large concrete dams. The long expected life and large mass of concrete dams and spillways tends to make them susceptible to gradual degradation mechanisms which begin in very small ways that are easy to miss, but can accelerate over time. Some of these mechanisms include freeze-thaw damage on the downstream face and crown, seepage under and around outflow conduits and spillways, slow-developing cracks in the dam interior, and erosion due to water flow and weathering. Each of these types of degradation can start out as a very minor problem, which sometimes can be present for

[1] Olson Engineering, Inc., Chief Engineer, Wheat Ridge, CO Larry.Olson@OlsonEngineering.com
[2] Olson Engineering, Inc., Project Geologist, Rockville, MD Lyndsay.Hazelwood@OlsonEngineering.com

years before being noticed. The presence of the initial degradation, however, tends to accelerate future problems. Freeze-thaw damaged surfaces hold more moisture than usual, leading to greater damage. Small cracks in the dam face become stress concentrators which lead to deeper cracking, while cracks which seep can lead to erosion and cracking due to the action of the water. Seepage under a spillway or around an outflow conduit slowly erodes the subgrade, leading to faster flow rates and even greater erosion rates.

The best defense a dam owner has against these threats is periodic inspection. Visual inspections, however, often only find problems after they have developed into major degradation. Some types of damage, such as voids under a spillway slab or cracking in the dam interior or on the upstream, submerged face, are very difficult or impossible to find with only visual means. This is where the use of Nondestructive Evaluation (NDE) techniques enters the picture. The various nondestructive methods available use stress waves, radio waves, and other types of low-level energy to penetrate through the concrete beyond what the eye can see. These methods can locate a void under a spillway, measure the depth of cracking and severity of freeze-thaw or other surface damage, and create an image slice through the interior of a dam to show cracks, debonded joints, and other degraded zones. Most of these methods can be done without dewatering the dam, and all are completely nondestructive and nonintrusive. In this paper, several of the NDE methods most commonly applied to dams will be discussed, along with example results from investigations of a number of dams.

NONDESTRUCTIVE EVALUATION (NDE) METHODS

While a number of NDE methods can be applied to the investigation of the condition of various concrete elements in a dam structure, there are five techniques that are particularly useful in most concrete dam investigations (Sack et al, 2013). The first technique discussed is the Spectral Analysis of Surface Waves (SASW) method, which is used for measuring the condition of concrete versus depth from the test surface as well as for crack depth measurement (Olson *et al.* 1994). The second method discussed is the Impact Echo (IE) method for evaluating concrete thickness and integrity from one accessible side on concrete dams, spillways and conduits. The third method discussed is the application of Ground Penetrating Radar (GPR) to spillway investigations. This method is used to map out voids and water seepage paths under a spillway, and will also provide information as to the spacing and depth of any reinforcing in the concrete for cases where this information is not known. The fourth method is Slab Impulse Response (SIR) which is sensitive to thin voids below spillway slabs and conduits and is used in conjunction with GPR. The fifth method is Sonic Velocity Tomography (SVT) which involves the use of sound wave transmission through a thin-arch dam interior to create a tomographic velocity image slice through the dam from upstream to downstream faces.

SPECTRAL ANALYSIS OF SURFACE WAVES (SASW) METHOD

The SASW method (ACI 228.2R-13) is based upon measuring surface waves propagating in layered elastic media and is illustrated in Fig. 1. The ratio of surface wave velocity to shear wave velocity varies with Poisson's ratio. However, reasonable estimates of

Poisson's ratio and mass density for concrete and other materials can normally be made with only a small effect on the accuracy of the shear wave velocity profile. Knowledge of the shear wave velocity combined with reasonable estimates of mass density of the material layers allows calculation of shear moduli for low-strain amplitudes. Surface wave (also termed Rayleigh; R-wave) velocity varies with frequency in layered media. A plot of this varying surface wave velocity versus wavelength is called a dispersion curve. The SASW tests and analyses are generally performed in three phases: (1) collection of data in situ; (2) construction of an experimental dispersion curve from the field data; and (3) forward modeling of the theoretical dispersion curve to match theoretical and experimental curves so that a shear wave velocity versus depth profile can be constructed.

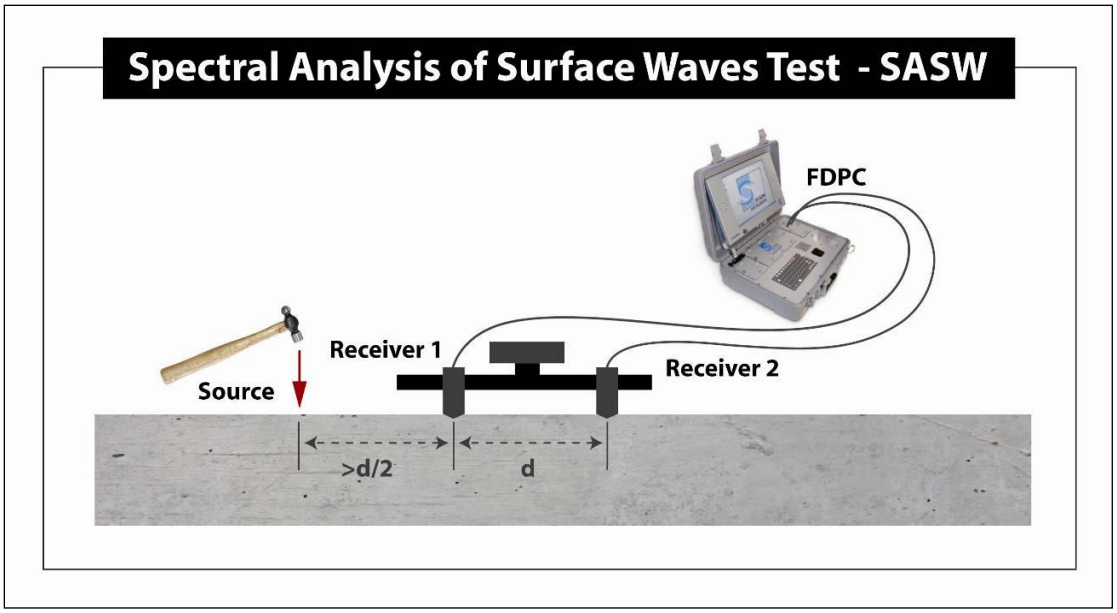

Figure 1. Typical SASW testing setup with source, receivers, and data collection system.

Collection of SASW Field Data

Typical SASW field tests are conducted with a pair of matched vibration transducers and an impact source. The transducers are typically displacement transducers or accelerometers mounted to or held in contact with the concrete surface. One example of an SASW data collection system is an Olson Instruments SASW-S test system, consisting of two displacement transducers mounted on a bar at a fixed spacing. The bar is pressed against the test surface, and impacts are made with a small hammer in line with the receivers. A photo of SASW data collection on a concrete dam face is shown in Fig. 2.

A data acquisition system such as the Olson Instruments Freedom Data PC is used to collect the waveforms from the two receivers and record the signal signals for spectral (frequency) analyses computerized signal conditioning and data acquisition system is then used to collect the waveforms from the two receivers and record the signals for spectral (frequency) analyses. The phase information of the transfer function (cross power spectrum) between the two receivers for each frequency is the key measurement.

Figure 2. SASW testing for possible freeze-thaw cracking damage on dam upstream face.

SASW Experimental Dispersion Curve Processing

Surface wave dispersion can be expressed in terms of a plot of surface wave velocity versus wavelength. This plot is called a dispersion curve plot. For sound concrete, the dispersion curve plot exhibits a constant velocity versus wavelength throughout the concrete thickness. If degradation or cracking present at the test location, the dispersion curve will have zones of lower velocity. The depth of the cracking or degradation can be estimated from the wavelength range of the dispersion curve.

The experimental dispersion curve is developed from the phase data from a given site by knowing the phase (N) at a given frequency (f) and then calculating the travel time (t) between receivers of that frequency/wavelength by:

$$t = N / 360*f \quad (1)$$

Surface wave (Rayleigh, R-wave) velocity (V_R) is obtained by dividing the receiver spacing (X) by the travel time at a frequency:

$$V_R = X / t \quad (2)$$

The wavelength (λ) is related to the velocity and frequency by:

$$V_R = f*\lambda \quad (3)$$

By repeating the above procedure for any given frequency using phase analyses functions, the surface wave velocity corresponding to a given wavelength is evaluated and the dispersion curve is determined. The phase data is typically viewed on the PC data acquisition system in the field to ensure that acceptable data is being collected. The phase data is then returned to the office for further processing. The phase of the cross power spectrum (transfer function) between the two receivers and the coherence function are used in creating the dispersion curves. After frequency masking of the phase record pair from the data set for each test location, an experimental field dispersion curve is developed that is the plot of surface wave velocity versus wavelength. This is illustrated in the software screen shot shown in Fig. 3 below.

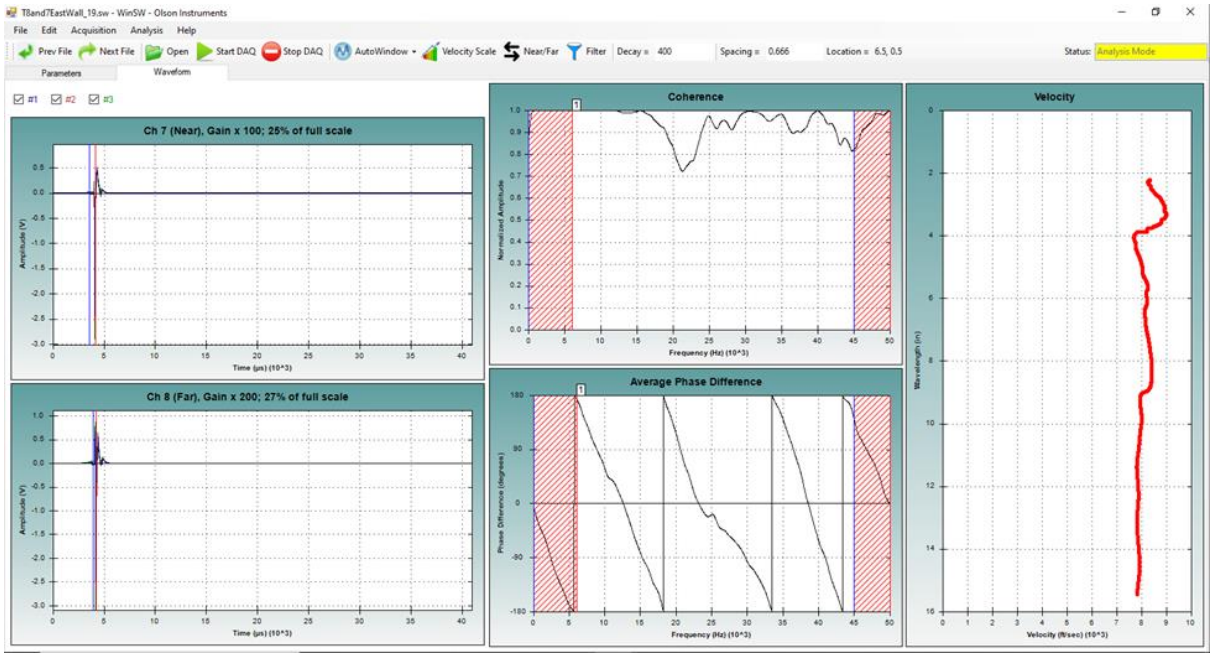

Figure 3. Example SASW data – Sound Concrete Conditions. Consistent surface wave velocity around 8,000 ft/sec is shown in the velocity vs. wavelength (dispersion curve) plot on the right. The time domain signals from the Channel 7 and Channel 8 SASW-S bar displacement transducers are shown on the left. The processed wrapped phase data from multiple impacts is in the bottom center plot and this data was analyzed to plot the dispersion curve. The top center plot shows the coherence between the two signals and it is typically above 0.9 near 1.0 up to a frequency of about 40,000 Hz which indicates good quality phase data.

Experimental dispersion curve data is presented in Fig. 4a from a test at a sound location on a dam face. This location showed no evidence of surface degradation from a visual inspection, and also showed no evidence of degradation in the SASW data results. Thus, this plot shows the relatively flat, high velocity (7,500 to 8,000 ft/s) dispersion curve typical of sound concrete and came from an area that was normally underwater and not subject to freeze-thaw damage cracking over time.

A second example data plot is presented in Fig. 4b. This is a plot from a test point that was below water in the summer but generally above water in the winter on the same dam face, where the 2- to 4-inch thick shotcrete repaired surface appeared to be distressed from freeze-thaw damage. The degradation of the concrete at the surface is supported by the SASW test results which showed a surface wave velocity of 5,500 ft/s at a wavelength of 4 inches (about the shotcrete depth) that decreased quickly to 3,700 ft/s to depths/ wavelengths of 22 inches. Since velocity to the 4th power is directly proportional to Young's elastic modulus squared is proportional to concrete strength (ACI 228.1R-89), this reduction in velocity reflects the freeze-thaw cracking damage effect on the much slower surface wave velocity and corresponding reductions in modulus and strength. Coring subsequently confirmed this was due to freeze-thaw cracking.

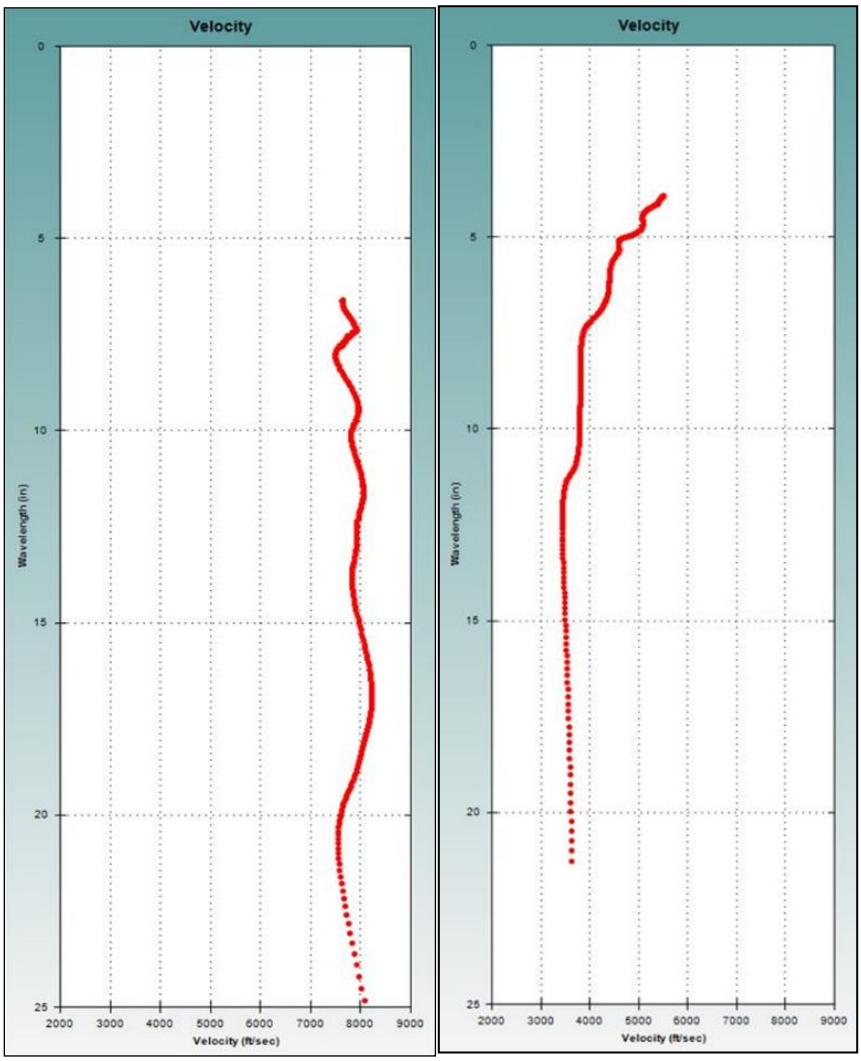

Figure 4. (Fig. 4a - left) SASW dispersion curves showing good surface wave velocity of 7,500 to 8,000 ft/s indicating "Sound" concrete conditions to at least 25 inches deep from surface, and (Fig. 4b - right) SASW dispersion curve showing a faster velocity of 5,500 ft/s at 4 inches deep decreasing to ~3,700 ft/s due to freeze-thaw cracking damage to a depth of 22+ inches.

IMPACT ECHO (IE) DISCUSSION

Impact Echo (IE) has also been used on dams with thicknesses of 10 ft or less to define the extent of cracking and concrete quality (Olson et al 1994). This one-sided access, resonance-based test is based on impacting the concrete and recording resonant echoes to indicate the thickness of elements as well as internal flaws such as void, cracking, and delamination in concrete.

Impact Echo (IE) Test Method

The IE method (ASTM C1383-15) involves hitting the concrete surface with a small solenoid impactor or ball-peen hammer and identifying the reflected wave energy with a displacement or accelerometer receiver mounted on the surface near the impact point. A simplified diagram of the method is presented in Figure 5 for a point-by-point test. The resulting displacement responses of the displacement receiver are recorded. The resonant echoes are usually not apparent in the time domain. The resonant echoes are more easily identified in the frequency domain. Consequently, the time domain test data are processed with a Fast Fourier Transform (FFT) which allows identification of frequency peaks (echoes). The displacement spectrum of the receiver or the transfer function (receiver displacement output/hammer force input vs. frequency) are used to determine the resonant peaks. If the thickness of a slab is known, the compression wave velocity (V_P) can be determined by the following equation:

$$V_P = 2*d*f/\beta \quad (4)$$

where d = slab thickness, f = resonant frequency peak. The above equation is modified by a β (Beta) factor of 0.96 for walls and slabs and typically written in terms of the echo depth as:

$$d = \beta*V_P/(2*f) \quad (5)$$

Where concrete thickness is not known or cannot be destructively determined in order to back-calculate a velocity from the echo, a typical IE factored P-wave velocity in concrete of 12,000 ft/s is used for ordinary structural concrete, and the resulting thickness is referred to as an "apparent thickness". SASW tests can also be used to calculate compressional wave velocity since for a concrete with a typical Poisson's ratio of 0.2:

$$V_P = V_R/0.56 \quad (6)$$

An example IE test record from sound concrete with a thickness of 12 inches is presented in Figure 6 below. The top plot is the time domain response of the displacement transducer to the solenoid impact. The lower plot is the Fast Fourier Transform of the time domain data that has a clear resonant echo peak corresponding to the 12-inch concrete thickness at this test location. An example IE test record showing delamination the results in a low-frequency flexural response is presented in Figure 7.

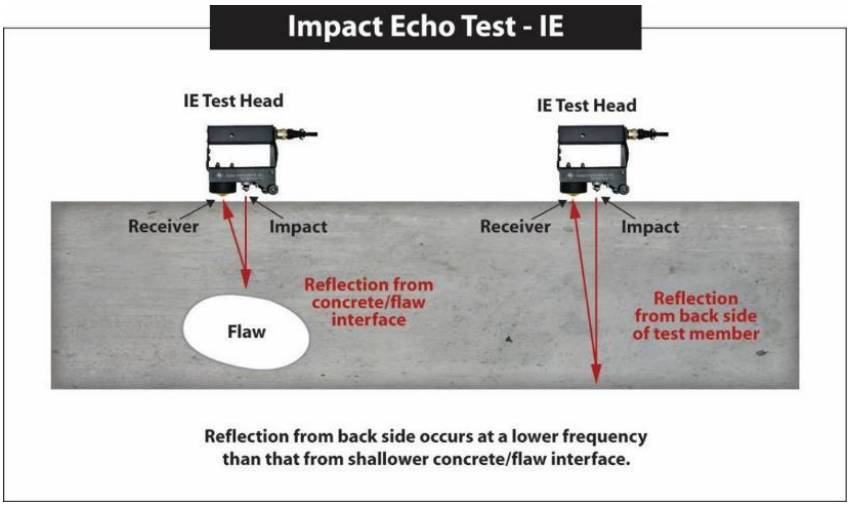

Figure 5. Impact Echo (IE) test method with built-in solenoid impactor and displacement transducer – note a ball peen hammer is used for concrete thicknesses of over 1 to 1.5 ft.

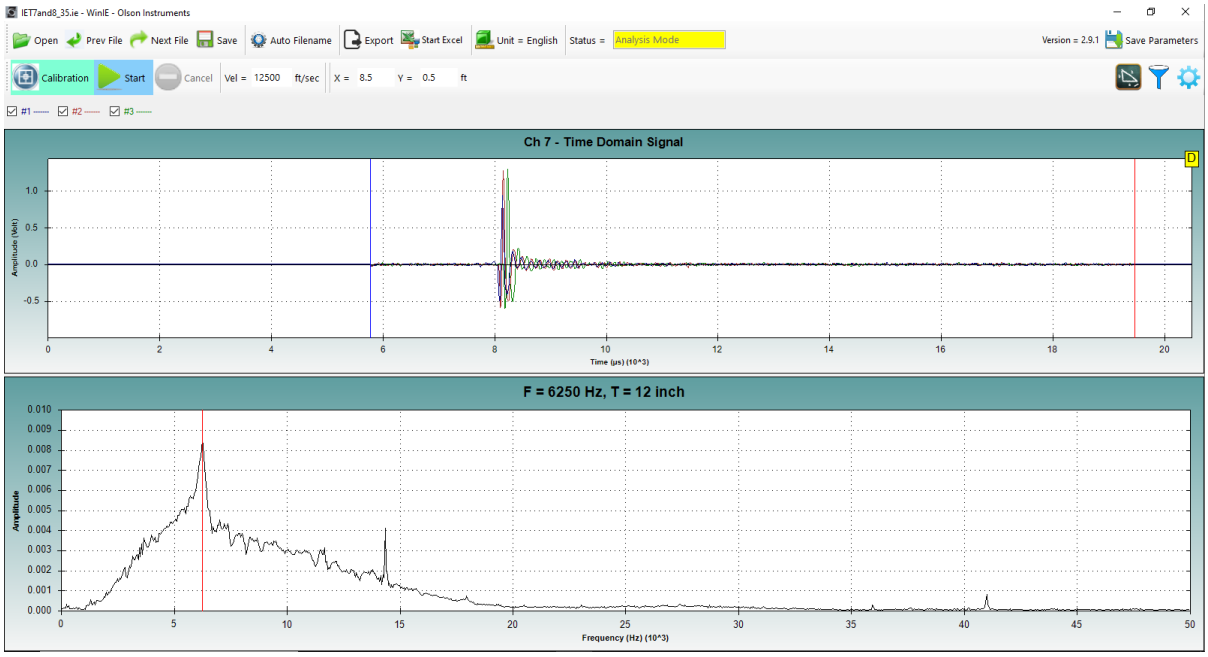

Figure 6. Example Impact Echo (IE) test data – Sound Conditions. The time domain signals from 3 impacts are shown in the top plot and the lower linear spectrum frequency domain plot has a strong single resonant echo peak at 6250 Hz that corresponds to a thickness of 12 inches for an IE velocity of 12,500 ft/s.

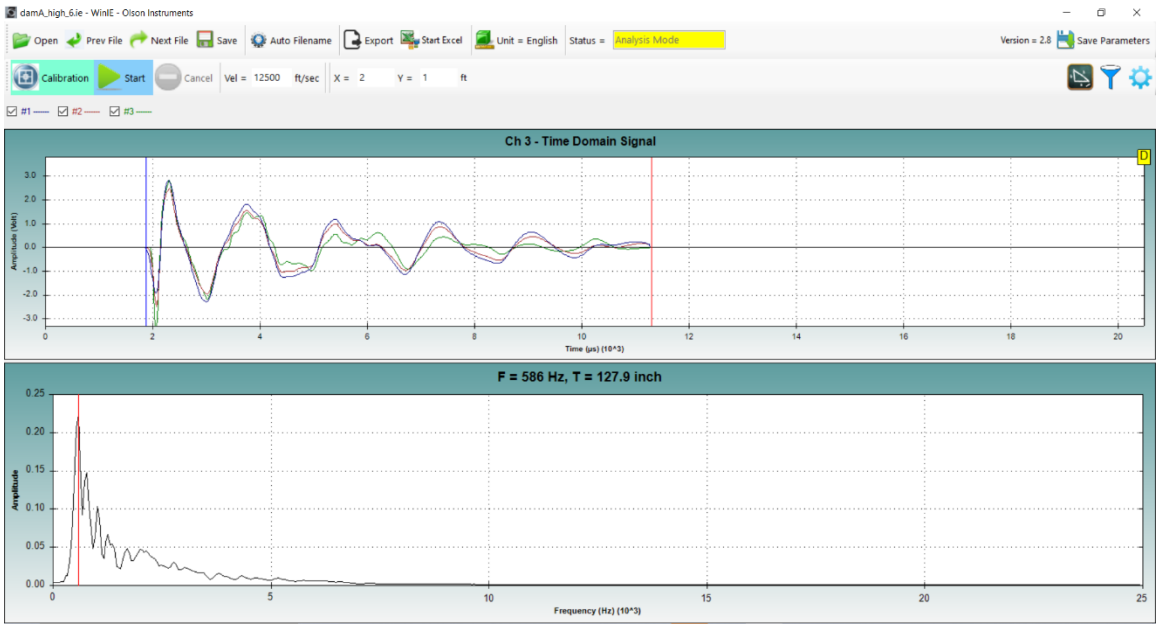

Figure 7. Example IE data – Poor Conditions due to delamination. The lower linear spectrum frequency plot shows an unrealistic thickness caluclation based on a low-frequency (dominant at 586 Hz) flexural resonance within a delamination. Note that the time domain plot above also shows a "ringing" signal for the same reason.

GROUND PENETRATING RADAR (GPR) METHOD

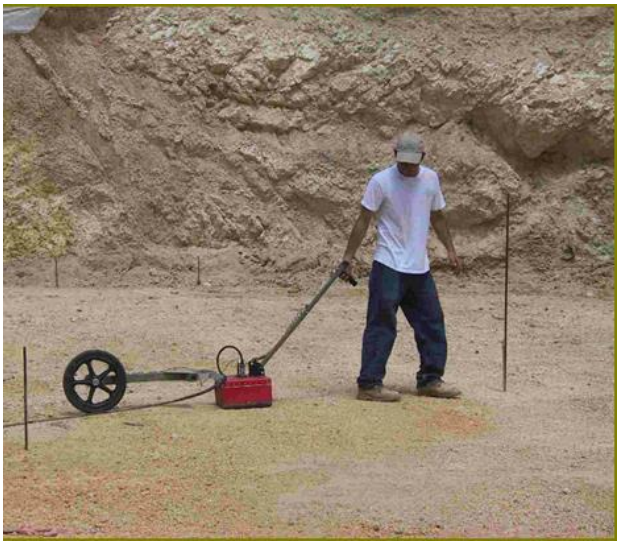

The GPR method (ACI 228.2R-13) involves moving an antenna across a test surface while periodically pulsing the antenna and recording the received echoes, as diagramed in Fig. 8 for a typical concrete slab. Pulses are sent out from the GPR computer driving the antenna at a frequency range centered on the design center frequency of the antenna, in this case 400 MegaHertz (MHz). These electromagnetic wave pulses propagate through the material directly under the antenna, with some energy reflecting back whenever the wave encounters a change in electrical impedance, such as at a rebar or other steel embedment or air-filled void. The antenna receives these echoes, which are amplified and filtered in the GPR computer, and then digitized and stored. A distance wheel records scan distance across the test surface and embedded features can be located as a given distance from the scan start position. For repetitive scanning, a standard survey is designed and adhered to as field conditions allow to minimize mistakes and to maximize data quality. Daniels (1996) expounds on the theory and application of the GPR method.

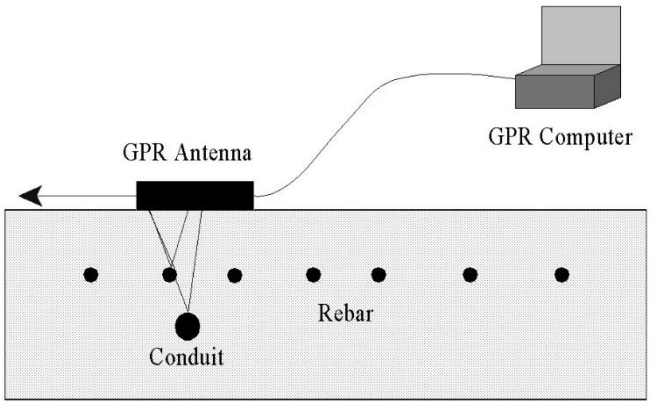

Figure 8. Ground Penetrating Radar (GPR) schematic and 400 MHz Antenna.

The scans for this investigation were created from pulses sent out at lateral intervals of near 48 pulses per foot. The resulting raw data is in the form of echo amplitude versus time. By inputting the dielectric constant (specific to the material being scanned; 9.8 was used for this investigation), and by estimating the signal zero point, the echo time data can be converted to echo depth. Concrete electromagnetic velocity (dielectric constant) calibration can be and in this case was performed using 8 spillway thickness values obtained from the cores taken. The scans are then typically plotted as waterfall plots of all of the individual data traces collected, with the lightness or darkness (or color) of each point in the plot being set by the amplitude and polarity (positive or negative) of the data at a given depth in each trace. Further, if data are collected along evenly spaced gridlines, a 3-D interpolation can be performed to generate a cubic display of data. This data cube can then be sliced along certain planes (typically XY, XZ, and YZ) to enhance recognition and display of target features. Also, amplitude threshold constraints can be set to allow display of GPR reflections within the given threshold values. Regional features are often more easily recognized when viewing a slice of 3-D interpolated data.

GPR Field Investigation and Example Data

To simplify field data collection for GPR (and Slab Impulse Response, SIR discussed in next section), a 4 x 4 ft grid was established at the spillway. A naming convention was used to designate each grid line in both the north-to-south and east-to-west directions. The centerline of the spillway, running longitudinally for more than 156 ft downstream (north), was named ‘C’. Longitudinal lines were designated at 4 ft intervals from right of center eastward as R1 through R6, and at 4 ft intervals from left of center westward as L1 through L6 when looking downstream from the spillway crest. The short east-to-west gridlines (axial lines) began with Line 1 located 2 ft downstream of the reservoir shore edge and continued at 4 ft intervals to line 40, approximately 158 ft downstream of the reservoir shore edge.

The GPR investigation was performed over a nominal length of 156 ft along the concrete spillway. All GPR data were collected using an antenna with a center frequency of 400 MHz and stored in a Geophysical Survey Systems Incorporated (GSSI) GPR field data collection system. The GPR scanning was performed in 13 lines along the length of

the spillway at lines spaced at 4 ft intervals. The actual scanning was split into 2 portions – upper and lower spillway. Initially, scanning was performed at the upper portion of the spillway, from the crest downstream to a distance of 120 ft (Line 30). Next, the lower spillway was scanned, from 116 ft (Line 30) to near 156 ft (Line 41) below the spillway crest. All GPR scans were started 2 ft from the reservoir shore edge and continued downstream. The spillway tapered down uniformly from upstream to downstream causing the two outside lines on both sides of the spillway (L6, L5, R5, and R6) to 'pinch out' at a distance less than 156 ft. The two outside scans on both sides of the spillway are shorter than the nine inside scans.

An example of GPR data recorded along the spillway center is presented in Figure 9. This is a waterfall plot of GPR data recorded along the centerline, 70 - 107 ft downstream of the spillway crest. The waterfall plot presented in the figure was manipulated and analyzed using a 2-D GPR analysis and display software package. Figure 9 shows 3 scan characteristics. The rebar mat ranges from a depth of 0.2 to 0.6 ft (depth in ft. on right hand vertical scale – left hand scale is time in nanoseconds). The slab bottom reflection is evident at a depth ranging from approximately 0.6 to 0.8 ft. The amplitude of the slab bottom reflection was used for void detection analysis with "bright" and "low" amplitude reflectors shown in Figure 9. Stronger negative amplitudes are indicative of a strong dielectric constant contrast (concrete to air), evidence of potential voids. The core location along the centerline, used for concrete dielectric constant calibration, is shown in the figure as well (near 96 ft). The concrete at this location measured 7.25 inches thick.

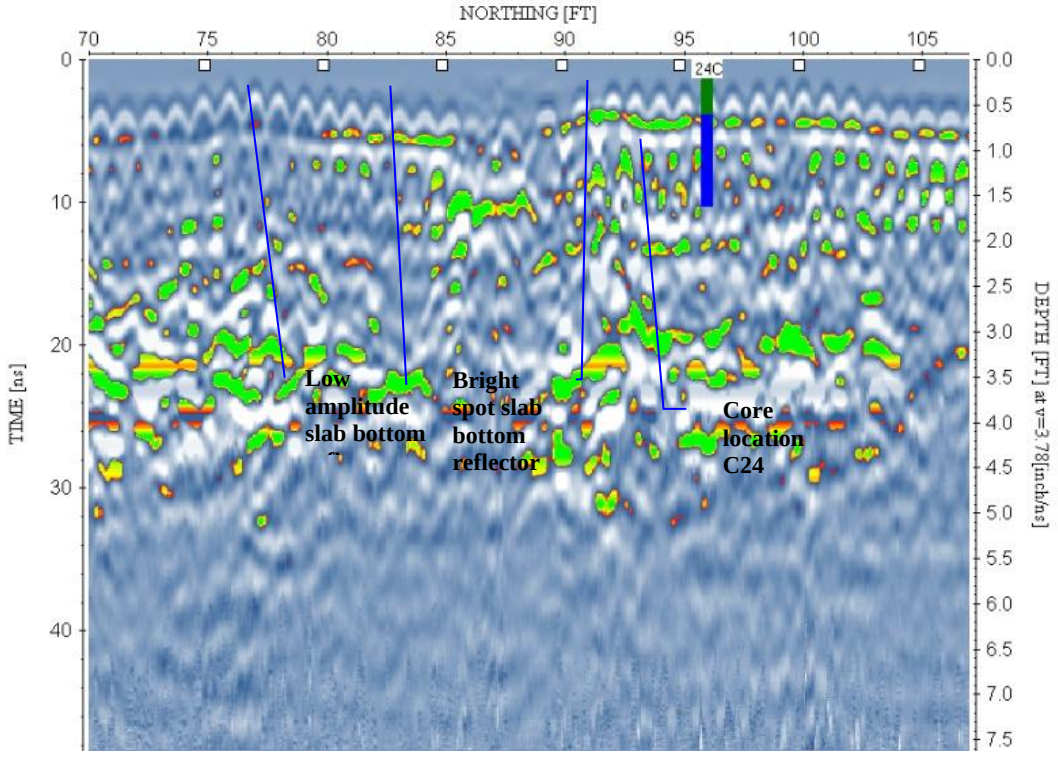

Figure 9. Example GPR data plot from the centerline, 70 – 107 ft below spillway crest.

SLAB IMPULSE RESPONSE (SIR) METHOD

The Slab Impulse Response (SIR) method (ASTM C1740-16) detects and defines the extent of good versus void/poor support conditions of a slab, but does not provide information on the depth or thickness of void (Fig. 10). The method was developed from a force-response vibration test for investigating the integrity of deep foundations and was originally adapted for a slab by a European group. The SIR investigation was conducted from the surface of the concrete spillway. Field equipment included an impulse hammer, Wilcoxon velocity transducer, and an Olson Instruments Freedom PC. The method involved hitting the concrete spillway to generate vibration energy. The 3-lb impulse hammer has a built-in load cell with a plastic head to measure the force of the impact. The vibration response of the concrete to the impact is measured with the velocity transducer held in contact with the concrete close to the point of impact. The outputs from 3 hits of the hammer and the receiver responses were viewed and recorded in the field and processed in the office.

The SIR data is processed on the PC with Fast Fourier Transform (FFT) Transfer Function operations on the time domain data to produce the mobility plots in frequency domain. Fig. 11 is an example plot of mobility (vibration velocity amplitude per pound force) as a function of frequency measured in cycles per second or Hertz (Hz) for good subgrade support (bottom plot). The low, and comparatively smooth, mobility is an indicator of good subgrade support conditions. Irregular and higher amplitude mobility indicates a less stiff more flexible slab-subgrade support system, indicating poor (void) support conditions as shown in Figure 12. The top plots in Figures 11 and 12 are of coherence and a value 0.9 to 1.0 indicates good quality data.

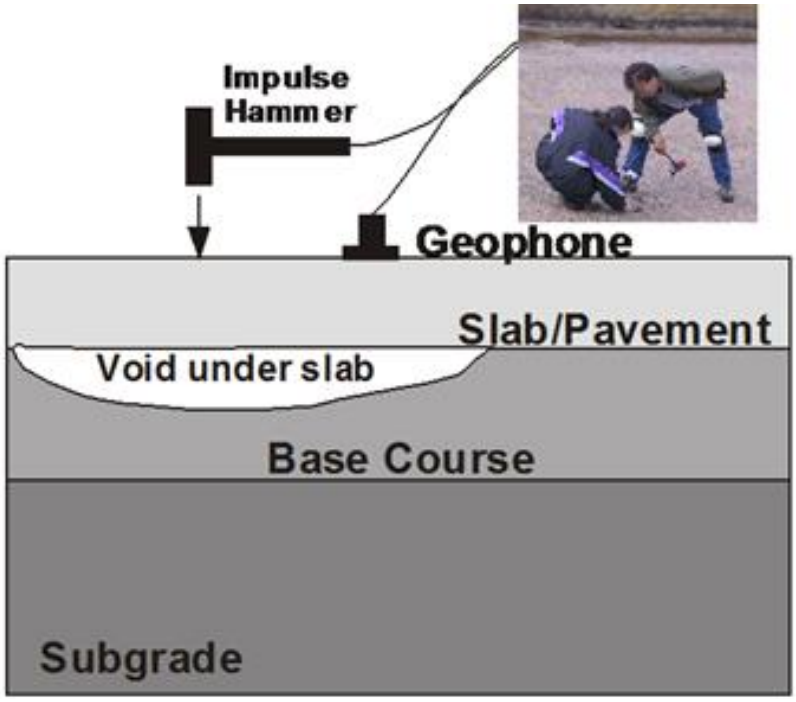

Figure 10. Slab Impulse Response Method (SIR).

Subgrade support condition evaluation is based on several measured parameters. First, the mean mobility (in/sec/lbf) provides a general indication of the spillway stiffness. Higher mobility may indicate a more flexible and less stiff spillway-subgrade system. Secondly, the shape of the mobility plot at frequencies above the initial straight-line portion of the curve (between 100 to 800 Hz in this investigation) is another indicator of subgrade support conditions. The response curve is more irregular and has a greater mobility for void versus good support conditions due to the decreased damping of the spillway vibration response for a void (Figure 12). Finally, the initial slope of the mobility plot gives the low-strain flexibility (in/lbf) of the spillway-subgrade system. The flexibility is a measurement of how much the spillway moves for a given impact, and the inverse of the flexibility is stiffness. Higher flexibility corresponds to less subgrade support or thinner concrete at the data point. Additional discussion of the SIR method and its history is given by Davis (2003).

Other factors typically considered in the SIR method include the geometry and thickness of the spillway, the boundary conditions in the vicinity of a test location (including cracks and joints), and the spillway reinforcement. Findings and conclusions on the spillway subgrade support conditions can usually be drawn based on SIR results, comparison of data from similar conditions, and/or by correlation with destructive (e.g., core) results. With other factors being constant, thinner spillways are more mobile and flexible than thicker spillways. Regardless of the thickness, the shape of a mobility curve from a point with good subgrade support is generally smooth with no low frequency peaks. The SIR method complements the GPR method in that it can detect very thin voids (less than 1/16 inch thick) while GPR generally detects voids of ¼-to ½-inch or greater in thickness.

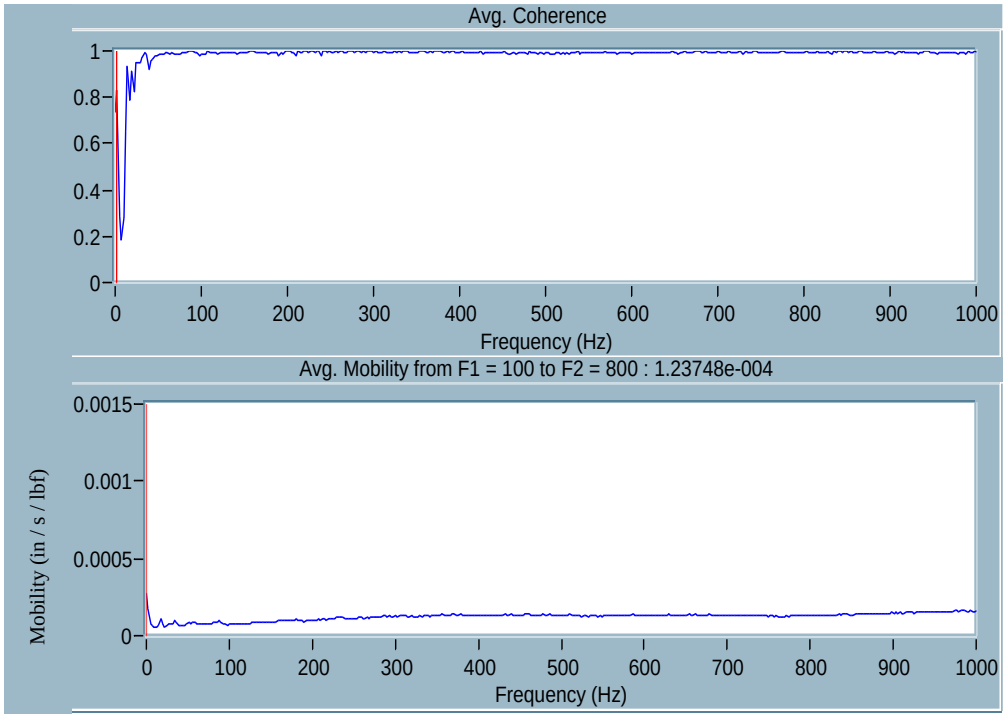

Figure 11. SIR Mobility for Good Subgrade Support with average mobility of 1.24E-04 in/s/lbf.

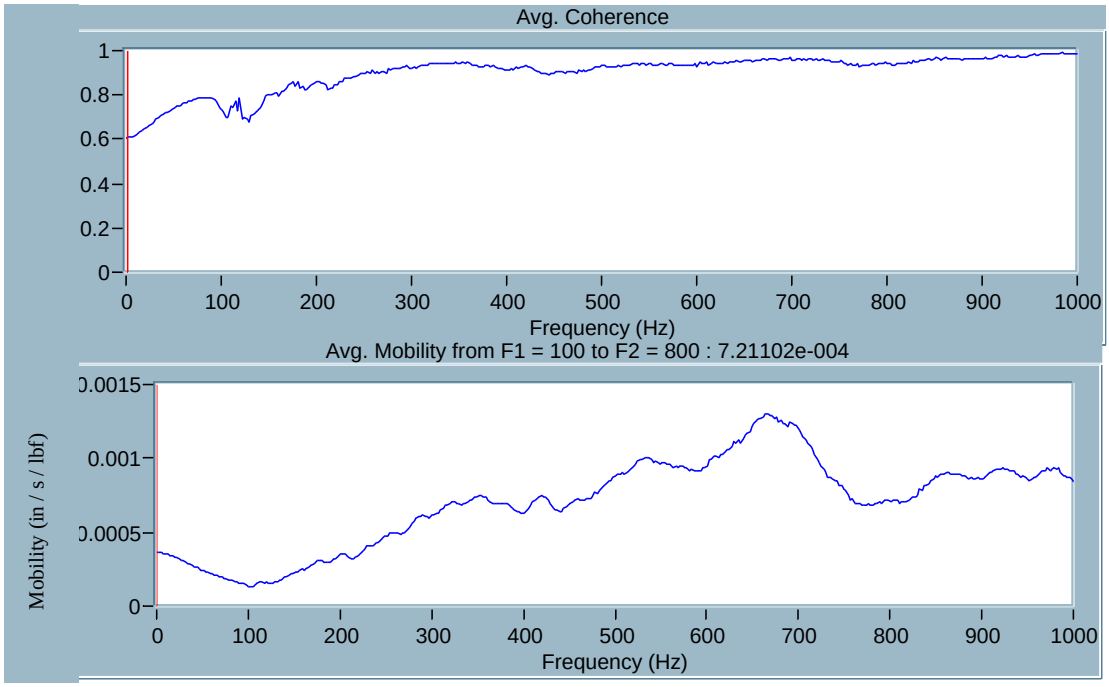

Figure 12. SIR Mobility for Void/Poor Subgrade Support with irregular, higher average mobility of 7.21E-04 in/s/lbf.

SIR Field Investigation

For the collection of the SIR data, 428 data points were taken along the spillway on a grid spaced at 4 ft intervals along the 156 ft tested length of the spillway, and over the entire width of the spillway. A nominally 4 x 4 ft grid was established at the spillway as described in the previous section and repeated herewith. A naming convention was used to designate each line in both directions. The centerline of the spillway, running longitudinally for more than 156 ft downstream, was named 'C'. Longitudinal lines were designated at 4 ft intervals from right of center eastward as R1 through R6, and at 4 ft intervals from left of center westward as L1 through L6 when looking downstream from the spillway crest. The short east-west trending lines (axial lines) began with Line 1 located 2 ft downstream of the reservoir shore edge and continued at 4 ft intervals to line 40, approximately 158 ft downstream of the reservoir shore edge. This grid system allowed for the generation of an image contour map that relates each location's mobility to the corresponding mean values of all SIR data collected at the site in a relative sense (see Figure 14 as discussed below). This image map was created from analyses of mobility and coherence plots.

Discussion of GPR and SIR NDE Results

The results of the NDE investigation are presented graphically in Figures 13 and 14 which presents plan and perspective views of 3-D GPR data showing strong amplitude slab bottom reflection values, an image map contouring the SIR relative mobility values, and the core locations with void thicknesses that were performed after the NDE investigation. The GPR and SIR results are discussed below.

GPR Results. After GPR data collection, the raw data were post-processed in our office to enhance target features and remove background and ambient noise. The digital processing steps for each scan on the upper portion of the spillway included 1) trace zeroing and 2) background noise removal. For the lower portion of the spillway, GPR data also underwent an automatic gain algorithm to normalize trace amplitude from scan to scan. The GPR data presented in Figure 13 (in both perspective and plan views) show the "bright", strong negative values for slab bottom reflection indicative of void and are the result of 3-D interpolation between the 13 lines scanned. The plots are separated into 2 sections, the upper and lower portions of the spillway. Areas of strong negative amplitude slab-bottom reflection or "bright spots" (red and orange shading in Figure 13) were interpreted as areas of potential voids. These bright spots are evidence of the strong contrast between the electrical properties of concrete and that of water or air-filled void versus the weaker contrast between the electrical properties of concrete and subgrade soil. From the GPR data, much of the spillway shows evidence of potential voids. The two largest areas are between 55 - 80 and 90 - 110 ft below the spillway crest. Smaller areas of potential void appear in Figure 13 as well. The GPR data did not allow for potential void thickness/depth approximation because of poor void bottom resolution; the core results provided this type of data. Core thicknesses were instrumental in confirming the NDE results and destructively measuring the spillway thickness and areas/thicknesses of void below the spillway slab.

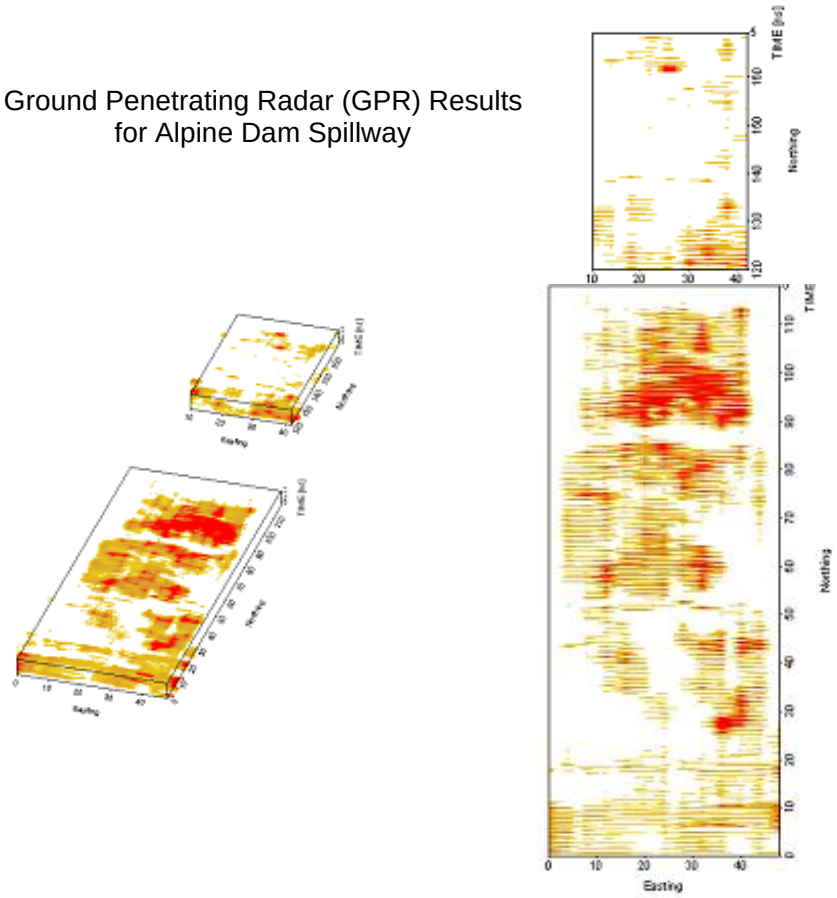

Figure 13. GPR results for Spillway Subgrade Void shown by brighter reflectors above.

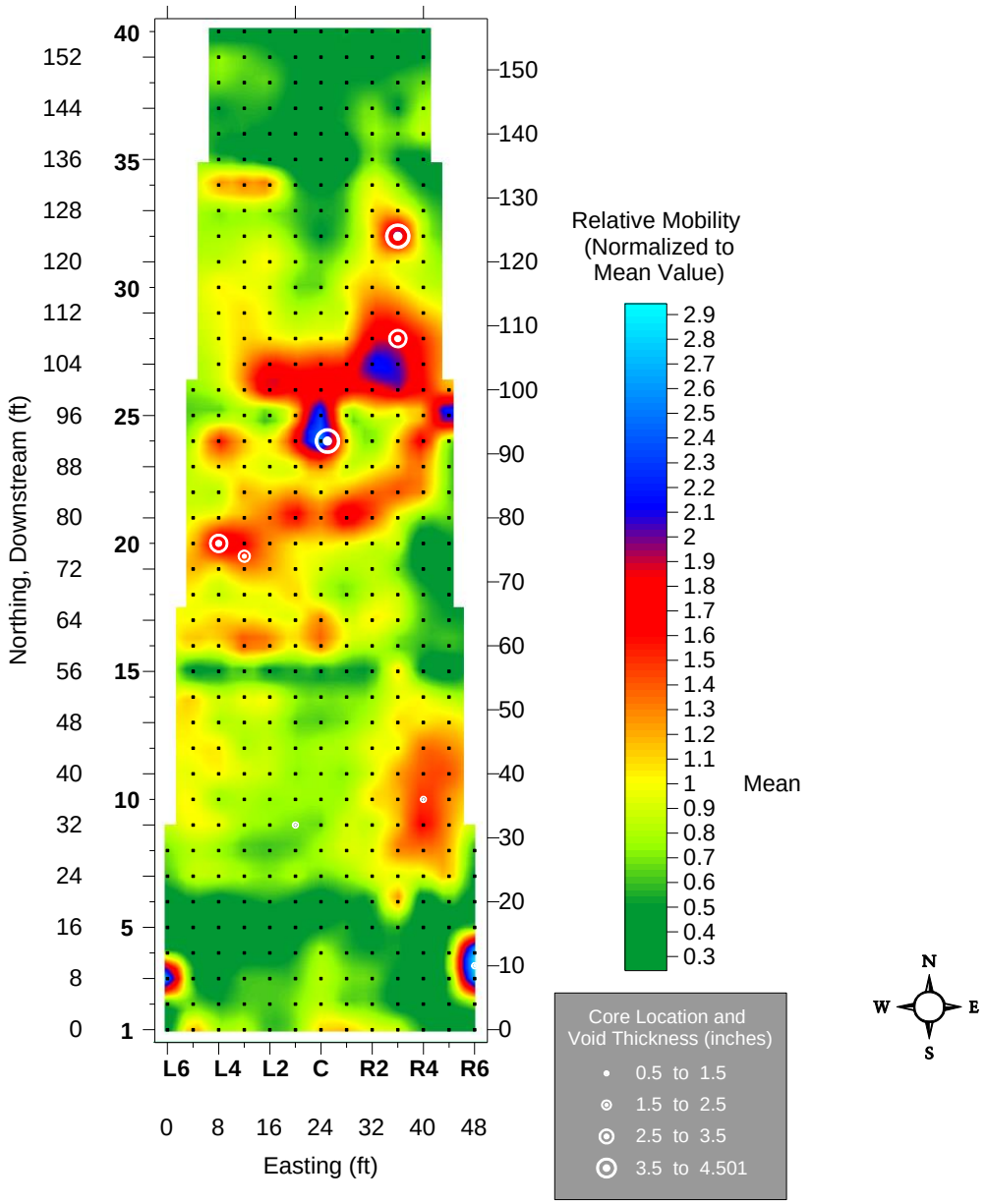

Figure 14. Slab Impulse Response (SIR) mobility results and Core location/void thicknesses.

SIR and Coring Results. The Slab Impulse Response (SIR) evaluation method is fundamentally used for the identification of potential shallow to deeper voids located within or directly below a concrete slab. The SIR method cannot identify the actual depth or thickness of a possible void, but can find the plan view location along an investigated portion of spillway in which a void might exist. From the SIR data performed on the spillway, an image contour map was created (Figure 14) relating the mobility of all data points to the spillway mean mobility value. These plotted values have been normalized to the mean mobility value recorded at the spillway. This image contour map in Figure 14 presents several sizeable areas for which the mobility is higher than the mean value for the spillway (bright yellow, red, and blue shades). The two largest and potentially most severe areas of void are between 55 - 80 and 90 - 110 ft

below the spillway crest (red and blue shades). Based solely on the SIR, these areas may indicate potential void beneath the spillway or may reflect a change in slab thickness. The coring results indicate that concrete thickness varies considerably over the length of the spillway. Comparisons of core data with mean mobility values confirmed small to large voids at SIR locations with normalized mobilities ranging from 0.6 and higher. Consequently, all SIR data points with normalized mobilities greater than 0.6 are likely to have poor subgrade to void support conditions. Even lower mobilities may have questionable support as no core encountered good support conditions.

Correlation of GPR and SIR Results. The GPR and SIR data correlate well as is evident from the plots presented in Figures 13 and 14, respectively. White areas in the GPR plots (weak amplitude slab bottom reflection) correspond to green areas (low mobility) in the SIR image map and suggest locations for better subgrade support. Figure 14 also includes the core locations and the depth of each void found. The coring results, shown in Figure 14 support the NDE data set results with void thicknesses ranging from 05 to 4.5 inches.

Correlation of GPR, SIR and Core Results. The GPR and Slab IR data correlate well as is evident from the plots presented in Figures 13 and 14. White areas in the GPR plots (weak amplitude slab bottom reflection) correspond to green areas (low mobility) in the Slab IR image map and suggest locations with better subgrade support. The coring results support the NDE data set results. Figure 14 plots the core locations and the size of each symbol relates to the thickness of the corresponding void. Voids were encountered for all locations cored, however, the thinner voids were found in areas of relatively low mobility (Slab IR) and weak slab bottom reflector (GPR). One exception was a core where a thin, 0.5 inch thick void was discovered. A proper explanation of this core may be the fact that significant voids are often closely surrounded by areas of good subgrade support, within a 3 to 5 foot radius. Even with NDE results to guide core location selection, coring can be a hit or miss operation. The correlated results infer that the Slab IR image map does indeed show locations of potential voids as opposed to changes in slab thickness. Video borescope probing was performed in the coreholes to provide visual confirmation of the NDE results. Both individual JPEG images as well as VHS recordings were obtained in each corehole. Figure 15 shows a borescope still-shot and the spillway concrete, void, and underlying subgrade are all evident in the photo. The images recorded with the video borescope showed voids extending from the coreholes and confirmed the NDE results for all drilled coreholes.

Figure 15. Borescope photo of slab subgrade void.

The combination of GPR and Slab IR was proven to be very successful in delineating subgrade voids at the alpine dam spillway. The combined methods also provide an accurate, fast, nondestructive, and inexpensive way to provide both qualitative and quantitative data regarding void location, size, and extent. The coring and corehole borescope investigation verified the accuracy of the NDE methods.

SONIC VELOCITY TOMOGRAPHY (SVT) METHOD

The Sonic Velocity Tomography (SVT) method is used to provide information on the interior structure and condition of concrete elements where access is available on two sides of the dam (Billington et al 2001). In general, a sonic energy impulse (e.g., from a hammer or solenoid impact) is imparted at a known location (source) and time (time zero), and the P-wave energy propagates through the structure and this test is known as Sonic Pulse Velocity (SPV):

$$SPV = t / d \quad (7)$$

where t = the travel time and d is the distance between the source and receiver. By placing an array of receivers (e.g., accelerometers above water or hydrophones below water) on the other side of the dam structure opposite from the energy source impacts, the arrival time of the P-waves can be recorded. Tomographic velocity data is then computed between each source impact point and receiver location based on the geometry of the structure and a matrix of P-wave raypaths and travel times at various angles through the structure as illustrated for a dam in Fig. 16 below.

The two major processing steps involved with P-wave tomography are first arrival picking and data inversion. The first arrival picking step consists of picking the time for each trace (signal) where the first-arrival of P-wave energy is observed at the receiver position and is shown in Fig. 17. After picking is complete, a 2D P-wave velocity model is then generated that best fits the first arrival picks by iteratively modifying a P-wave

velocity grid model until the misfit between the modeled and real travel time values is minimized, subject to smoothing constraints. P-wave tomography results provide an image of the internal conditions of the tested structure and can be used to identify the size, shape and location of defects (i.e., low velocity zones).

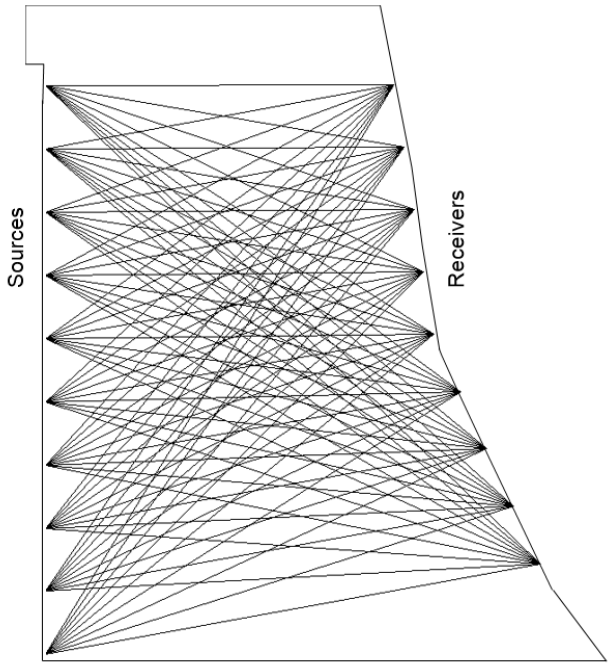

Figure 16. SPV test raypaths for Source (upstream) and Receiver Locations.

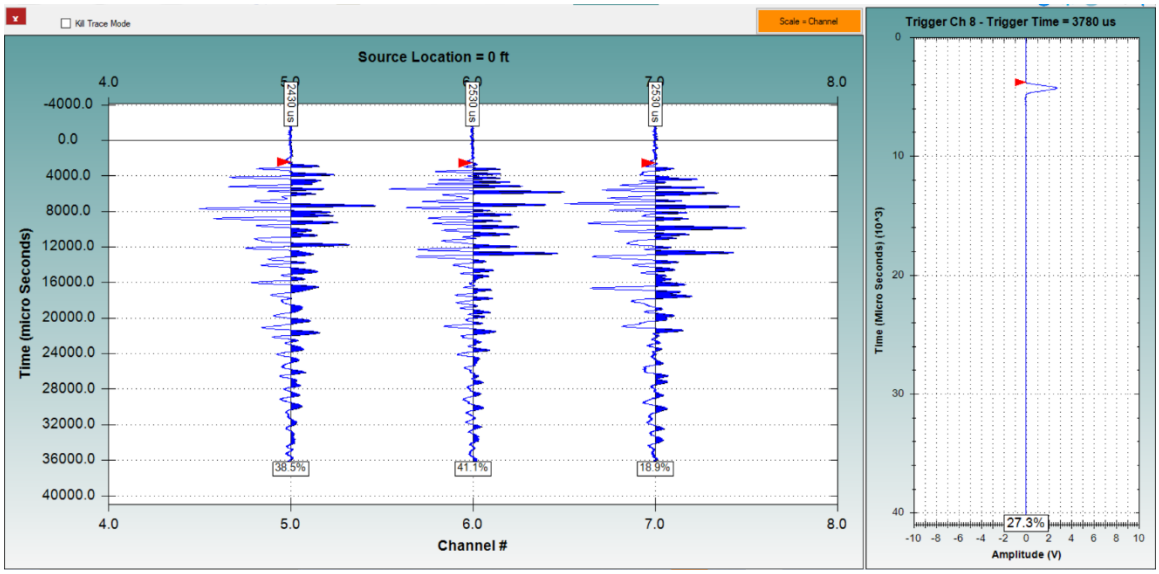

Figure 17. Example SPV data in which the first arrival times of P-wave signals from 3 revievers (channels) are shown by the red arrows in the left plot. The right plot shows the hammer signal and the inital impact time at the red arrow.

Typically, tomographic images are analyzed to look at the velocity changes within the concrete. Areas with lower velocity correspond to typically internally cracked and thus weaker, damaged concrete, while areas with higher velocities are considered to be

sounder and stronger concrete. The results can also show areas with cracking damage or other discontinuities in concrete. It should be noted that in tomographic analysis, it is also possible to get what are called "artifacts" in the data in areas with low ray density (not many data paths passing through an area) or in areas with non-linear or non-homogeneous velocities.

The SVT analysis results shown in Figure 18 provide a picture of the interior condition of the concrete through a slice of the dam from the downstream to upstream faces. These results show generally sound concrete below elevation 88 ft and lower velocities indicative of freeze-thaw cracking damage above 88 ft with the slowest velocities generally at the upstream face. It should be noted that in this particular example, these results were consistent with SASW results where the majority of test points with slow velocities at depth were located at 90 feet or above on a 5-foot test grid. This portion of the dam was more exposed to winter freezing conditions as it was above the water levels in winter time. Concrete compressional wave velocities of 12,000 to 15,000+ ft/s are indicative of good to excellent quality concrete. Slower velocities are due to freeze-thaw cracking damage.

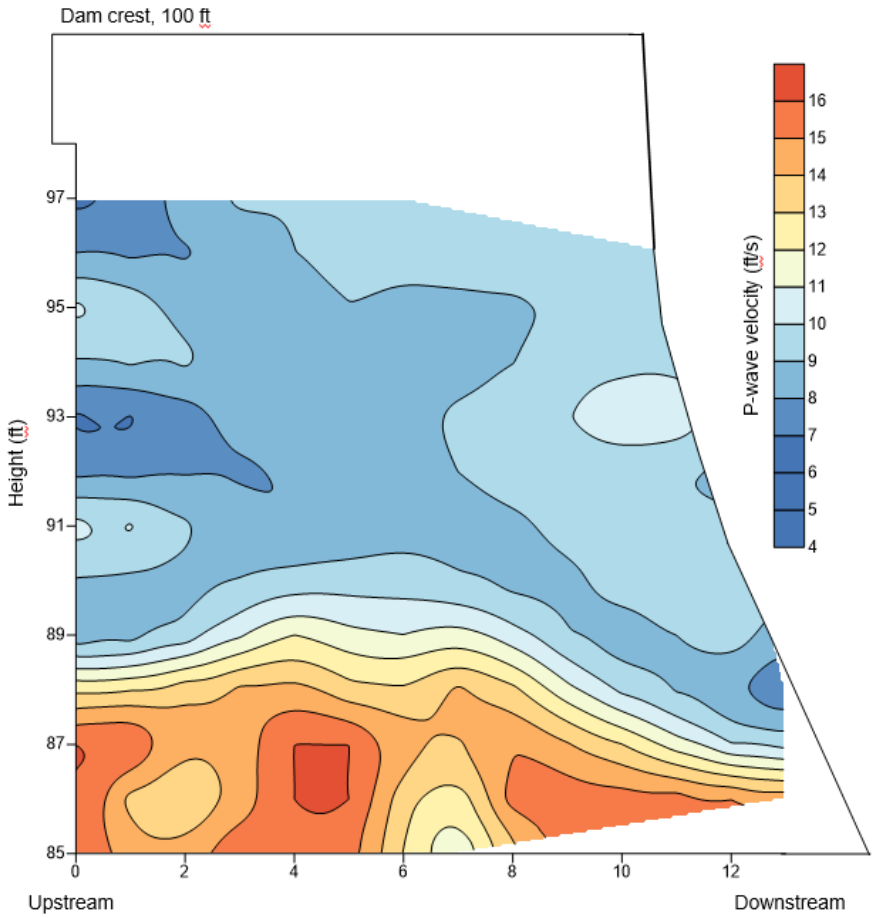

P-Wave Velocity in 1000's of ft/s

Figure 18. Sonic Velocity Tomogram with distance scales in ft. Note that slower velocities of 4,000 to 10,000 ft/s are indicative of moderate to severe freeze-thaw cracking damage and occur above elev. 88 ft with the slowest velocities at the upstream face (left side). Velocities below 88 ft were higher and indicative of sound concrete.

CONCLUSIONS ON CONCRETE DAM NDE

Several methods for NDE investigations of concrete dam elements have been presented, each of which can provide information on damage and degradation not available from a simple visual inspection. The methods presented include SASW tests for surface damage and crack depth, GPR for rebar location and GPR and SIR for spillway slab subgrade void location, and SVT tests to survey the entire cross-section of a dam interior and reference to IE tests as well.

Spectral Analysis of Surface Waves (SASW) testing was used to map the lateral extent and the depth of degradation that is often associated with freeze-thaw cracking damage. SASW is typically done above water on exposed dam surfaces with no significant preparation required of the dam faces or crest. The results from this testing can greatly benefit the owners and operators by identifying the depth and extent of minor degradation before it becomes a major problem. SASW testing can also determine the depths of cracks perpendicular to the surface by testing across them.

Impact Echo (IE) testing is complementary to SASW testing and sensitive to cracking damage that is sub-parallel to parallel to the concrete test surface. Impact Echo has also been found to be useful for cracking/void/thickness NDE on concrete dam elements up to 10 ft in thickness. Note that if needed both SASW and IE testing can be done below water with waterproofed equipment and divers.

Ground Penetrating Radar (GPR) is an electromagnetic method and was used to determine the location/depth of steel reinforcement in the spillway and provide insight on the lateral extent of thicker subgrade voids (< ¼ to ½ inch thick). The location of reinforcement is a crucial exercise for retrofitting a spillway. Identifying the subgrade voids at an early stage will provide the owners and operators with the information necessary to solve minor erosion/settlement problems before they become serious issues.

The combination of GPR and Slab Impulse Response (SIR) NDE was proven to be successful in delineating thin voids of less than 0.25 inch (SIR only) to thicker subgrade voids (SIR and GPR) at the alpine dam spillway. The SIR and GPR methods also provide a fast, nondestructive, and inexpensive way to provide both qualitative and quantitative data regarding void location, size, and extent. The coring and corehole borescope investigation verified the accuracy of the NDE methods. The NDE results were used to target the cores in questionable to poor to void support. Coring should be performed for confirmation of NDE to validate the data and identify areas in need of grouting repairs as well as to determine void thicknesses.

Sonic Pulse Velocity (SPV) testing with crossing raypaths from upstream to downstream is used to apply Sonic Velocity Tomography (SVT) to analyze the internal cross-section of the dam. The velocity tomograms provide insight into the low velocity/low strength/freeze-thaw cracked (or Alkali-Silica Reaction cracking damage) areas that may have been previously only visually identified on the surface. However, the extent of low strength/damaged/cracked concrete inside a dam is generally unknown until SPV testing

and SVT data analyses are performed. The information gained from the velocity tomograms allows concrete dam owners and dam engineers to identify the extent of weak/damaged areas and assess the safety of the dam and the need for repairs.

The NDE methods presented are all completely nondestructive and non-invasive, and usually can be applied to dams without dewatering or other interference with normal operations. Together, these methods provide a powerful set of tools that can be used by owners and operators of dams and similar facilities to identify where repairs are needed and ensure that the structures in their care continue to safely perform the service for which they were originally constructed. Each of these technologies provides insight to individual problems recognized by visual inspection. When NDE methods are combined and analyzed as appropriate for a given dam project along with destructive coring and laboratory investigations, they provide the owner and operator with the information essential for assessing the concrete condition/integrity, longevity and structural safety throughout the dam, spillways and conduits.

REFERENCES

ACI 228.1R-89 Report In-Place Methods for Determination of Strength of Concrete, American Concrete Institute Manual of Concrete Practice (1989).

ACI 228.R-13 Report Nondestructive Test Methods for Evaluation of Concrete in Structures, American Concrete Institute Manual of Concrete Practice (2013).

Billington, E.D., Sack, D.A., & Olson, L.D., 2001. Sonic Pulse Velocity Testing to Assess Condition of a Concrete Dam, SAGEEP Conference Proceedings on Geophysical Engineering, Denver, Colorado.

Daniels, D.J., 1996. Surface-penetrating radar IEE UK.

Davis, A.G., 2003. The Nondestructive Impulse Response Test in North America: 1985-2001, NDT&E International, Elsevier Science.

Hollema, D. & Olson, L.D. 2004. Application of a Combined Nondestructive Evaluation Approach to Detecting Subgrade Voids Below a Dam Spillway, SAGEEP Conference Proceedings on Geophysical Engineering, Colorado Springs, Colorado.

Olson, L.D., Chan, Y.F., Sack, D.A., Dumont, M.F., Gilmore, R.T., and Christy, J.T., 1994. "The Use of Impact-Echo and Spectral-Analysis-of-Surface-Wave Methods for the Concrete Investigation of the Rogers Dam Spillway Structure", Proceedings of the 56th American Power Conference, Chicago, Illinois.

Sack, D.A. and Olson, L.D., 2013. "Integrated Dam Condition Evaluation Using A Synergy of Nondestructive and Locally Destructive Techniques with Analytic Tools To Improve Dam Safety", HydroVision International 2013, July 2013.